

## *Supporting Information*

# AIE Active Polyelectrolyte Based Photosensitizers: The Effects of Structure on Antibiotic-Resistant Bacterial Sensing and Killing, and Pollutant Decomposition

Hui Xie,<sup>a</sup> Wanshan Hu,<sup>b</sup> Fei Zhang,<sup>a</sup> Tingting Peng,<sup>\*b</sup> Caizhen Zhu<sup>\*a</sup> and Jian Xu<sup>a</sup>

<sup>a</sup> Institute of Low-Dimensional Materials Genome Initiative, College of chemistry and environmental engineering, Shenzhen University, Shenzhen 518060, China. E-mail: czzhu@szu.edu.cn.

<sup>b</sup> College of Pharmacy, Jinan University, Guangzhou 510632, China. E-mail: pengtt@jnu.edu.cn

†Electronic Supplementary Information (ESI) available: See DOI:  
10.1039/x0xx00000x.

## Experimental Procedures

### Materials and Methods

**Materials.** 4-bromobenzophenone, pyridin-4-ylboronic acid, 4-vinylpyridine, potassium carbonate ( $K_2CO_3$ ), palladium acetate ( $Pd(OAc)_2$ ), Triphenylphosphine ( $P(C_6H_5)_3$ ), triethylamine (TEA), 1,4-dibromobutane, 1,6-dibromohexane, titanium tetrachloride ( $TiCl_4$ ), dimethylformamide (DMF), Tetrahydrofuran (THF), methylene blue (MB), methyl orange (MO), rhodamine B (RhB), and 9,10-anthracenediyl-bis(methylene)-dimalonic acid (ABDA) were obtained from Macklin. tetrakis(triphenylphosphine)palladium(0) ( $Pd[P(C_6H_5)_3]_4$ ), zinc dust, rose bengal (RB), and phosphate buffer saline (PBS) were purchased from Aladdin. They were used without further purification unless otherwise stated. Luria-Bertani (LB) broth and LB agar were from USB Co. Methicillin-resistant *S. epidermidis* (MRSE) was obtained from the General Microbiological Culture Collection Center of China.

**Measurements.** NMR spectra were determined on a Bruker 400NMR spectrometer with tetramethylsilane (TMS,  $\delta = 0$  ppm) as an internal standard. High-resolution mass spectra (HRMS) were performed on Waters Xevo TQD with an ESI source. UV–visible absorption (UV) spectra were recorded on the Shimadzu UV-2550 spectrometer. Photoluminescence (PL) spectra were measured using HITACHI F7000 Fluorescence Spectrophotometer. Dynamic light scattering (DLS) measurements were performed using a Malvern Nano-ZS instrument at room temperature. The morphology of the molecule was observed using a Transmission Electron Microscope (TEM, JEOL JSM-6700F). The bacterial morphology was observed by Scanning Electron Microscopy (SEM, JEOL JSM-7800F). The Zeta potential of the sample was measured by the Malvern Zetasizer Nano ZS90 (Malvern Instrument, UK) instrument at room temperature. The fluorescence photos were taken Confocal Laser Scanning Microscopy (CLSM, LEICA SP8).

**Computational method.** The geometries of ground-state molecules were fully optimized by the hybrid B3LYP combined with the 6-31G (d, p) basis set. The excited-

state characteristics were calculated by the time-dependent density functional theory (TD-DFT) using optimized ground state geometries. To examine the performance of the free pyridine unit (BP unit) and 4-vinylpyridine unit (BVP unit) as rotational molecular rotors in **DBPEs** and **DBPVEs**, respectively, cluster models with different torsion angles are constructed based on these two molecules. In the two models of four arms, BP and BVP units in **DBPEs** and **DBPVEs** were fixed, respectively, and the other three arms were fixed. The energy changes of torsion angles ( $\Delta E_T$ ) from 0° to 180° in axisymmetric BP and BVP units were scanned at 10° intervals, and other intramolecular rotations and vibrations were ignored. Gaussian 16 package (Revision D.01) was used in all the calculations.

**ROS detection vis chemical method.** To study the ROS generation efficiency of **DBPE-4**, **DBPE-6**, **DBPVE-4**, and **DBPVE-6**, ABDA was used to detect the ROS generation upon light irradiation. The ABDA solution (concentration = 100  $\mu\text{M}$ ) was mixed with different compounds (concentration = 10  $\mu\text{M}$ ) in water and exposed to light irradiation (400-700 nm) at a power of 60 mW  $\text{cm}^{-2}$  for different times. The decomposition of ABDA was monitored by ultraviolet spectrometry at 378 nm.

**ROS quantum yield measurements.** The ROS quantum yield of different compounds in water ( $\Phi$ ) was measured using ABDA as an indicator and Bengal rose (RB) as a standard reference. Taking **DBPE-4** as an example, the ROS quantum yield is calculated using the following equation:

$$\Phi_{\text{DBPE-4}} = \frac{\Phi_{\text{RB}}(K_{\text{DBPE-4}} \cdot A_{\text{RB}})}{K_{\text{RB}} \cdot A_{\text{DBPE-4}}}$$

Where  $K_{\text{DBPE-4}}$  and  $K_{\text{RB}}$  are the decomposition rate constants of the photosensitizing process determined by the plot  $\ln(A_0/A)$  versus irradiation time.  $A_0$  is the initial absorbance of ABDA while  $A$  is the ABDA absorbance after different irradiation times.  $A_{\text{DBPE-4}}$  and  $A_{\text{RB}}$  represent the light absorbed by **DBPE-4** and RB, which are determined by the integration of the absorption bands in the wavelength range of 400-700 nm.  $\Phi_{\text{RB}}$  is the ROS quantum yield of RB, which is 0.75 in water. The calculation method of ROS quantum yield of **DBPE-6**, **DBPVE-4** and **DBPVE-6** is the same as that of

#### **DBPE-4.**

**Bacterial Culturing.** MRSE was cultured according to the ATCC protocols/specifications. A single colony of bacteria on solid culture medium [Luria broth (LB) for MRSE] was transferred to 5 mL of liquid culture medium and grown at 37 °C for 16 h. Bacteria were harvested by centrifuging and washed by PBS for three times. The supernatant was discarded and the remaining MRSE was resuspended in PBS and diluted to an optical density of  $10^6$  colony-forming unit (CFU) at 600 nm ( $1 \text{ OD}_{600} = 10^6 \text{ CFU mL}^{-1}$ ) for subsequent tests.

**Confocal laser scanning microscopy (CLSM) characterization.** Bacteria suspensions ( $\text{OD}_{600} = 1.0$ ) were incubated with 10  $\mu\text{M}$  of **DBPVE-4** under dark condition for 2 h at 37°C. Individual aliquots of 1  $\mu\text{L}$  of the pre-prepared mixed suspensions were added to paraformaldehyde pretreated glass slides followed by slightly covering coverslips for immobilization. The specimens were examined by confocal laser scanning microscopy using a 405 nm laser. The fluorescence of **DBPVE-4** was highlighted in red. The experimental conditions and operations of **DBPVE-6** towards microbes were totally the same as that of **DBVPE-4**.

**Zeta potential measurement.** MRSE was incubated with concentration gradient from 0 to 10  $\mu\text{M}$  of **DBPVE-4** at 37°C for 2 h, respectively. The samples were harvested by centrifugation, followed by resuspension in deionized water for Zeta potential measurements with Nano-ZS. The bacteria without **DBPVE-4** treatment was used as a control. The experimental conditions and operations of **DBPVE-6** towards microbes were similar to those of **DBPVE-4**.

**Antibacterial Experiments.** The antibacterial performance of **DBPVB-4** was evaluated *via* the CFU counting method. Bacterial suspension ( $\text{OD}_{600} = 1.0$ ) and **DBPVE-4** with concentration gradient from 0 to 10  $\mu\text{M}$  were added to 96 well plate and then irradiated with white light ( $60 \text{ mW cm}^{-2}$ , 30 min). Bacteria without **DBPVE-4** or white light treatment were used as control group. After that, the bacterial suspension was diluted to  $1 \times 10^5$  times with PBS, and inoculated on LB agar plate, for 16h

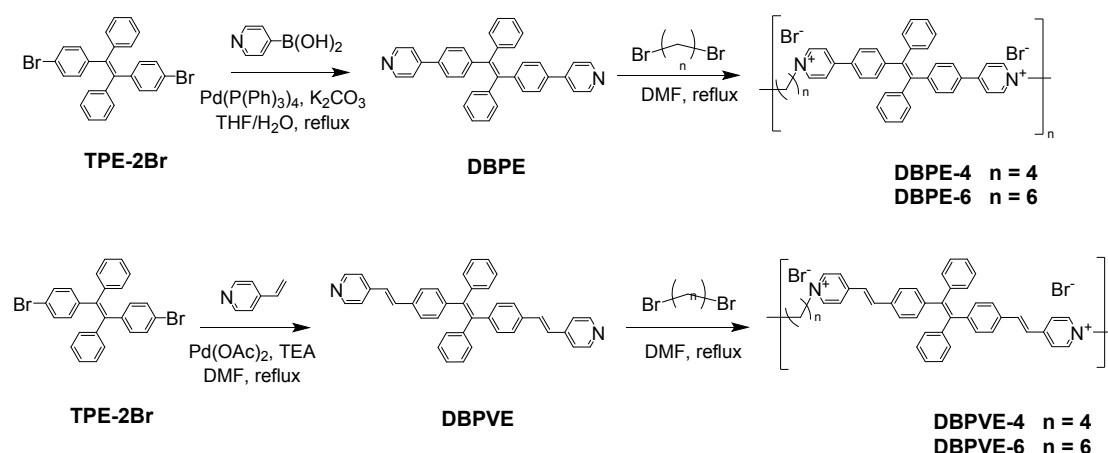
incubation. The diameter of the solid agar plates was 90 mm. The bacterial inhibition ratio (IR) was calculated under light and dark conditions according to the following equation:

$$IR = \frac{C_0 - C}{C_0} \times 100\%$$

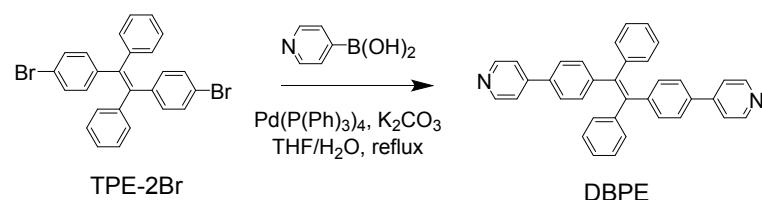
Where  $C$  is the CFU of the experimental group treated by **DBPVB-4** and  $C_0$  is the CFU of the control group without incubation with **DBPVB-4**. The experimental conditions and operations of **DBPVE-6** towards microbes were totally the same as that of **DBPVE-4**.

**Scanning electron microscopy (SEM) measurements.** The bacterial suspension (OD<sub>600</sub> = 1.0) was incubated with 10 μM **DBPE-4** in 50 mM PBS, and then the cells were irradiated with white light (60 mW cm<sup>-2</sup>, 30 min). The bacterial treated with **DBPVE-4** with and without light irradiation were chosen as control groups. The resulted cell suspension was dropped into fresh silicon slices for further drying in the air. After drying, 0.1% glutaraldehyde was used to fix cells for 1 h and the high concentration of glutaraldehyde (0.5%) was added for further 2h-fixing. After washing by sterile water, the specimens were dehydrated by the addition of ethanol in a graded series (50% for 5 min, 70% for 5 min, 90% for 5 min, and 100% for 5 min) and naturally dried under air. The specimens were gold-coated for SEM examination. The experimental conditions and operations of **DBPVE-6** towards microbes were totally the same as that of **DBPVE-4**.

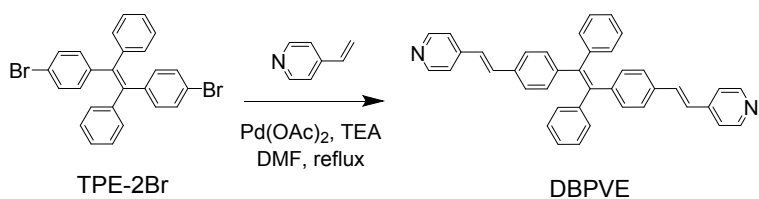
## Synthesis



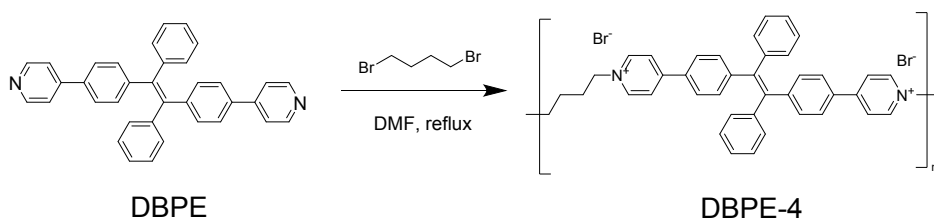
**Scheme S1.** The synthesis routes of **DBPE-4**, **DBPE-6**, **DBPVE-4** and **DBPVE-6**.



**Synthesis of 1,2-Diphenyl-1,2-bis(4-(pyridin-4-yl)phenyl)ethane (DBPE).** TPE-containing precursor 1,2-bis(4-bromophenyl)-1,2-diphenylethane was synthesized according to previously literature.<sup>1</sup> 1,2-bis(4-bromophenyl)-1,2-diphenylethane (489 g mol<sup>-1</sup>, 1.02 mmol, 500 mg), pyridin-4-ylboronic acid (123 g mol<sup>-1</sup>, 3.06 mmol, 376.3 mg), Pd[P(C<sub>6</sub>H<sub>5</sub>)<sub>3</sub>]<sub>4</sub> (1155 g mol<sup>-1</sup>, 0.102 mmol, 117.9 mg), and K<sub>2</sub>CO<sub>3</sub> (138 g mol<sup>-1</sup>, 4 mmol, 552 mg) were dissolved in mixture of THF and H<sub>2</sub>O (30 mL, V<sub>THF</sub>:V<sub>water</sub> = 2:1). Then, the mixture was refluxed at 120 °C for 24 h under argon protection, and then stirred for another 30 min at room temperature. The solvent was removed using rotary evaporator and filtered with CH<sub>2</sub>Cl<sub>2</sub>. The filtrate was removed using rotary evaporator and resultant crude compound was purified by silica gel column chromatography with hexane/ethyl acetate by volume of 3:1 to obtain the yellow pure **DBPE** with 55.5% yield. <sup>1</sup>H NMR (400 MHz, CDCl<sub>3</sub>-d) δ 8.55-8.54 (d, J = 5.6 Hz, 4H), 7.45-7.44 (d, J = 2.8 Hz, 4H), 7.37-7.35 (d, J = 8 Hz, 4H) 7.14-6.99 (m, 14H) ppm. <sup>13</sup>C NMR (100 MHz, CDCl<sub>3</sub>-d) δ 150.10, 149.13, 147.52, 144.48, 143.09, 140.77, 135.85, 135.14, 132.00, 131.25, 127.89, 127.74, 126.74, 126.23, 125.11, 125.05, 124.85, 121.18 ppm. HRMS (ESI) *m/z*: Calcd for C<sub>36</sub>H<sub>27</sub>N<sub>2</sub>: 487.2169, found: 487.2170.

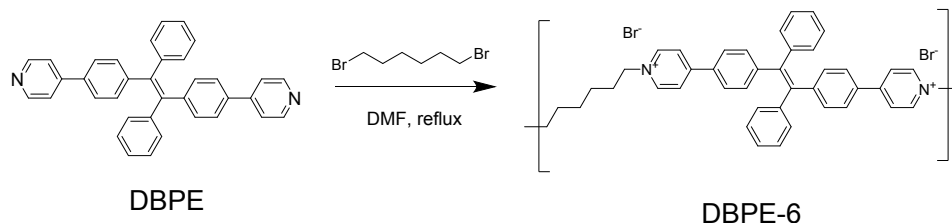


**Synthesis of 1,2-diphenyl-1,2-bis(4-((E)-2-(pyridin-4-yl)vinyl)phenyl)ethene (DBPVE).** 1,2-Bis(4-bromophenyl)-1,2-diphenylethene ( $489 \text{ g mol}^{-1}$ , 1.02 mmol, 500 mg), 4-vinylpyridine ( $105 \text{ g mol}^{-1}$ , 3.06 mmol, 0.642 g),  $\text{Pd(OAc)}_2$  ( $224 \text{ g mol}^{-1}$ , 0.0408 mmol, 9.16 mg),  $\text{P(C}_6\text{H}_5)_3$  ( $262.3 \text{ g mol}^{-1}$ , 0.163 mmol, 42.7 mg) and 9 mL dry TEA were dissolved in 30 mL DMF and placed in a 100 mL flask. Then, the mixture was refluxed at  $80 \text{ }^\circ\text{C}$  for 36 h under argon protection, and then stirred for another 30 min at room temperature. The solvent was removed using rotary evaporator. The resultant crude compound was purified by silica gel column chromatography with hexane/ethyl acetate by volume of 1:1 to obtain the yellow pure **DBPVE** with 67.8% yield.  $^1\text{H NMR}$  (400 MHz,  $\text{CDCl}_3$ -*d*)  $\delta$  8.50-8.49 (d,  $J=4 \text{ Hz}$ , 4H), 7.40-7.39 (d,  $J=2.4 \text{ Hz}$ , 4H), 7.28 (s, 2H), 7.25-7.25(d,  $J=2.8 \text{ Hz}$ , 4H), 7.07-7.03 (m, 6H), 7.00-6.92 (m, 8H), 6.88 (s, 2H) ppm.  $^{13}\text{C NMR}$  (100 MHz,  $\text{CDCl}_3$ -*d*)  $\delta$  150.10, 144.63, 144.34, 143.28, 140.90, 134.31, 134.00, 133.98, 132.81, 131.88, 131.85, 131.37, 127.92, 127.78, 126.82, 126.74, 126.52, 126.39, 125.70, 120.76 ppm. HRMS (ESI)  $m/z$ : Calcd for  $\text{C}_{40}\text{H}_{31}\text{N}_2$ : 539.2482, found: 539.2483.

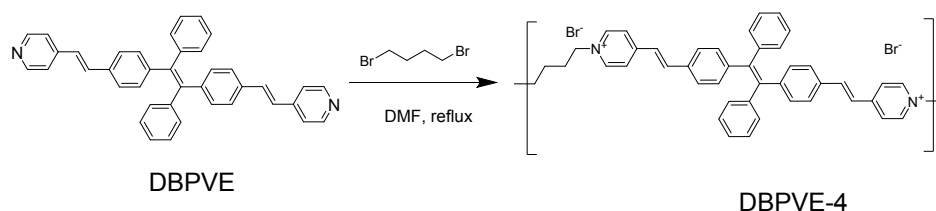


**Synthesis of DBPE-4.** A Schlenk tube was charged with **DBPE** ( $487 \text{ g mol}^{-1}$ , 0.288 mmol, 140 mg) and 10 mL DMF. and then 1,4-dibromobutane ( $216 \text{ g mol}^{-1}$ , 0.288 mmol, 62.2 mg) were added into each Schlenk tube, respectively. The mixture was refluxed at  $80 \text{ }^\circ\text{C}$  for 36 h under argon protection and then stirred for another 30 min at room temperature. The solvent was removed using rotary evaporator. All products were washed by 10 mL THF and 10 mL hexane for 5 times to obtain the corresponding.

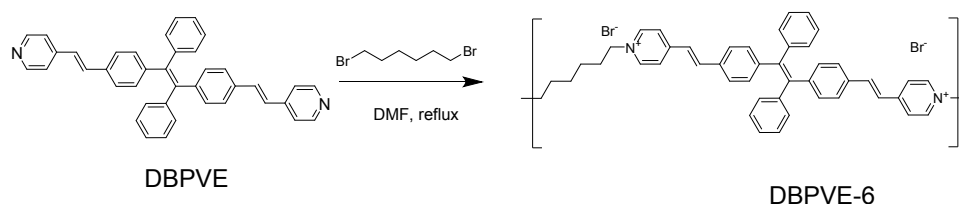
cationic polymer **DBPE-4** as a yellow solid with 44.2% yield.  $^1\text{H}$  NMR (400 MHz,  $\text{DMSO-}d_6$ )  $\delta$  9.45-8.13 (br, 8H), 8.05-6.50 (br, 18H), 4.75-4.57 (br, 3H), 2.02-0.86 (br, 6H) ppm.



**Synthesis of DBPE-6.** **DBPE-6** was obtained as a yellow solid with 50.8% yield using a similar synthetic procedure as **DBPE-4**, starting from **DBPE** ( $487 \text{ g mol}^{-1}$ , 0.288 mmol, 140 mg), 1,6-dibromohexane ( $244 \text{ g mol}^{-1}$ , 0.288 mmol, 70.3 mg) and DMF (10 ml).  $^1\text{H}$  NMR (400 MHz,  $\text{DMSO-}d_6$ )  $\delta$  9.25-8.13 (br, 8H), 8.00-6.75 (br, 18H), 4.67-4.53 (br, 3H), 2.02-1.00 (br, 10H) ppm.



**Synthesis of DBPVE-4.** **DBPVE-4** was isolated as an orange solid with 58.1% yield. The synthetic process of **DBPVE-4** was similar to **DBPE-4**, starting from **DBPVE** ( $539 \text{ g mol}^{-1}$ , 0.270 mmol, 145 mg), 1,4-dibromobutane ( $216 \text{ g mol}^{-1}$ , 0.270 mmol, 58.3 mg) and DMF (10 ml).  $^1\text{H}$  NMR (400 MHz,  $\text{DMSO-}d_6$ )  $\delta$  9.30-7.69 (br, 12H), 7.68-6.83 (br, 18H), 4.64-4.48 (br, 3H), 1.67-0.83 (br, 6H) ppm.



**Synthesis of DBPVE-6.** **DBPVE-6** was isolated as an orange solid with 57.8% yield. The synthetic process of **DBPVE-6** was similar to **DBPE-4**, starting from **DBPVE** ( $539 \text{ g mol}^{-1}$ , 0.270 mmol, 145 mg), 1,6-dibromohexane ( $244 \text{ g mol}^{-1}$ , 0.270 mmol, 65.9 mg) and DMF (10 ml).  $^1\text{H}$  NMR (400 MHz,  $\text{DMSO-}d_6$ )  $\delta$  9.30-7.69 (br, 12H), 7.68-6.83 (br, 18H), 4.64-4.48 (br, 3H), 1.67-0.83 (br, 6H) ppm.



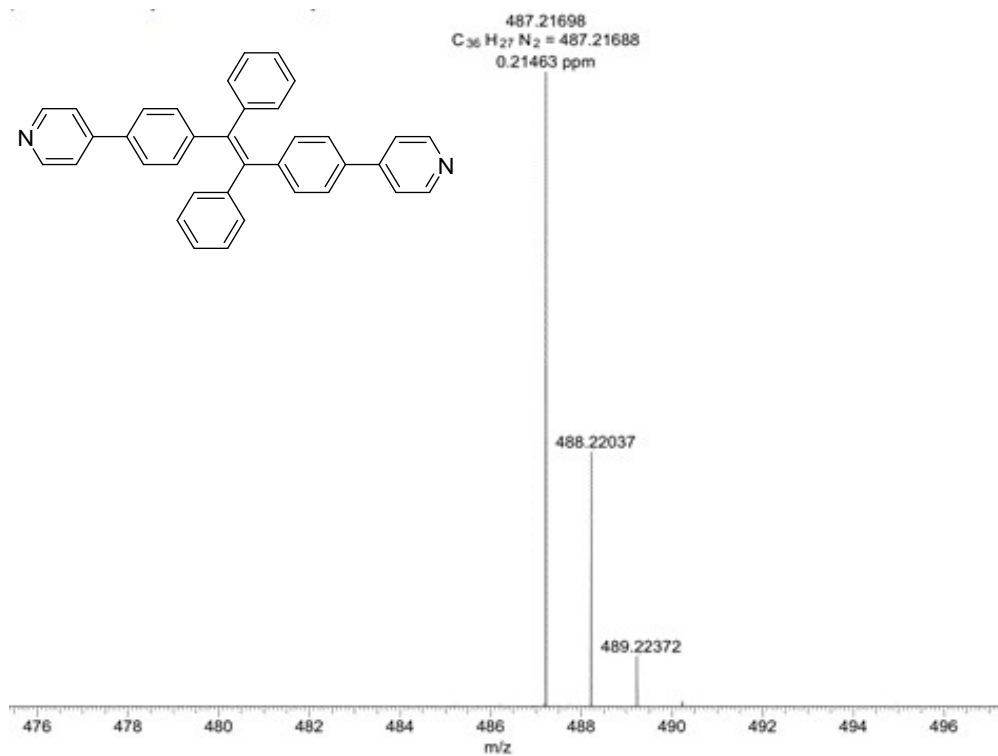


Figure S3. ESI-Mass spectrum of compound of DBPE.

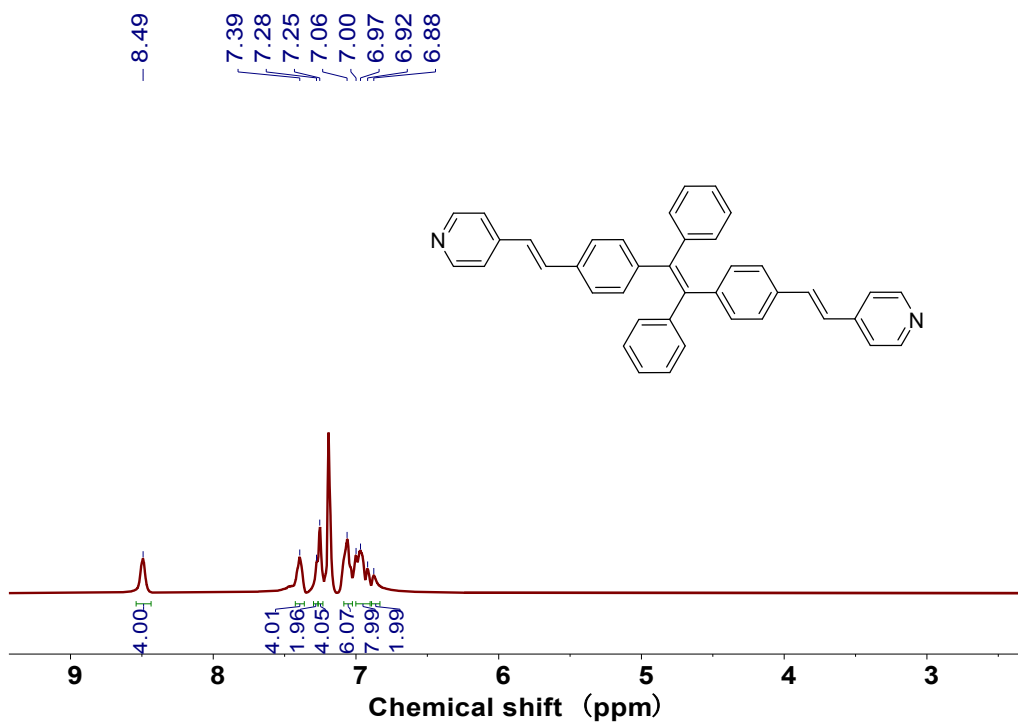


Figure S4. <sup>1</sup>H NMR spectrum of DBPVE.

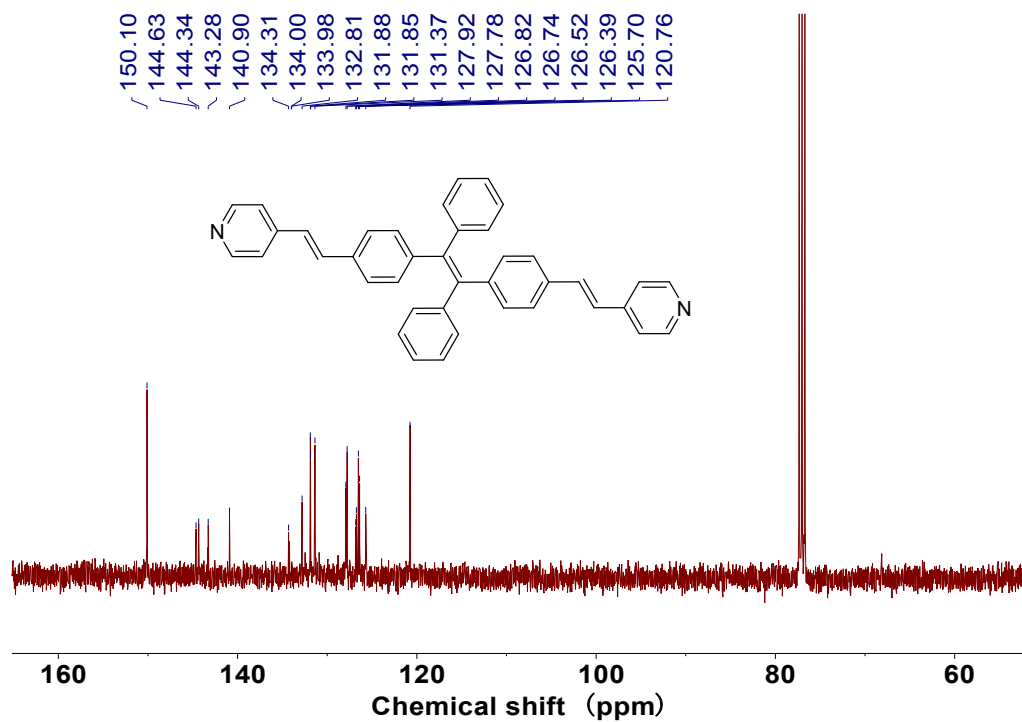


Figure S5.  $^{13}\text{C}$  NMR spectrum of DBPVE.

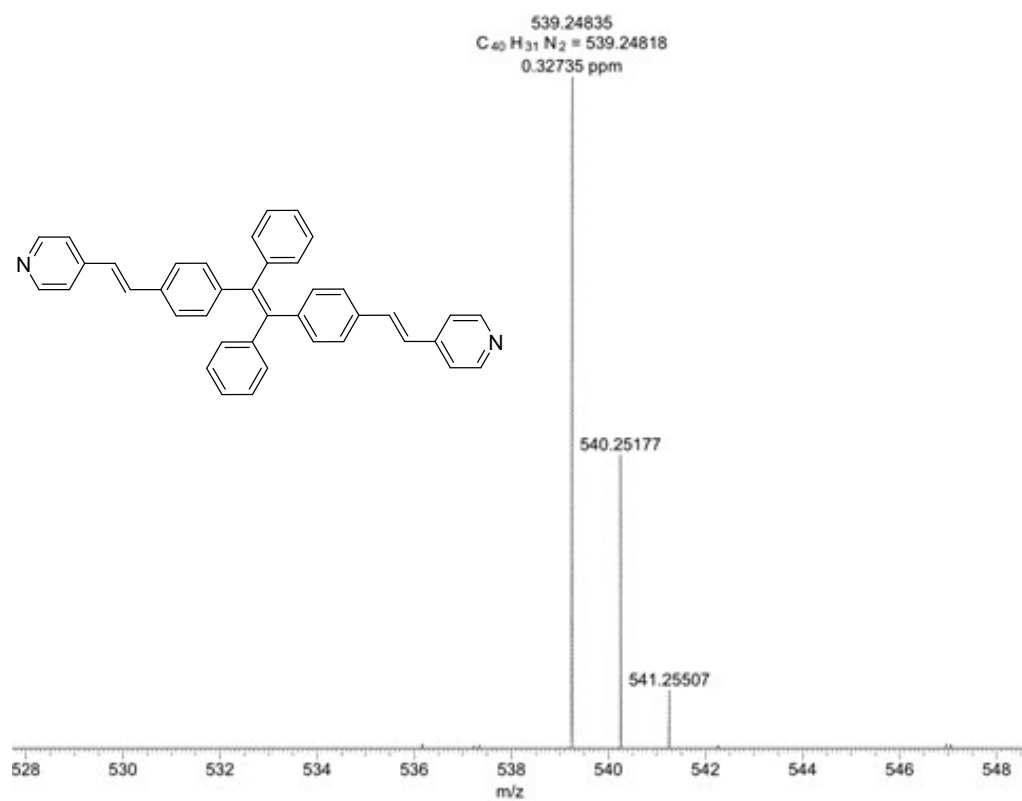


Figure S6. ESI-Mass spectrum of compound of DBPVE.

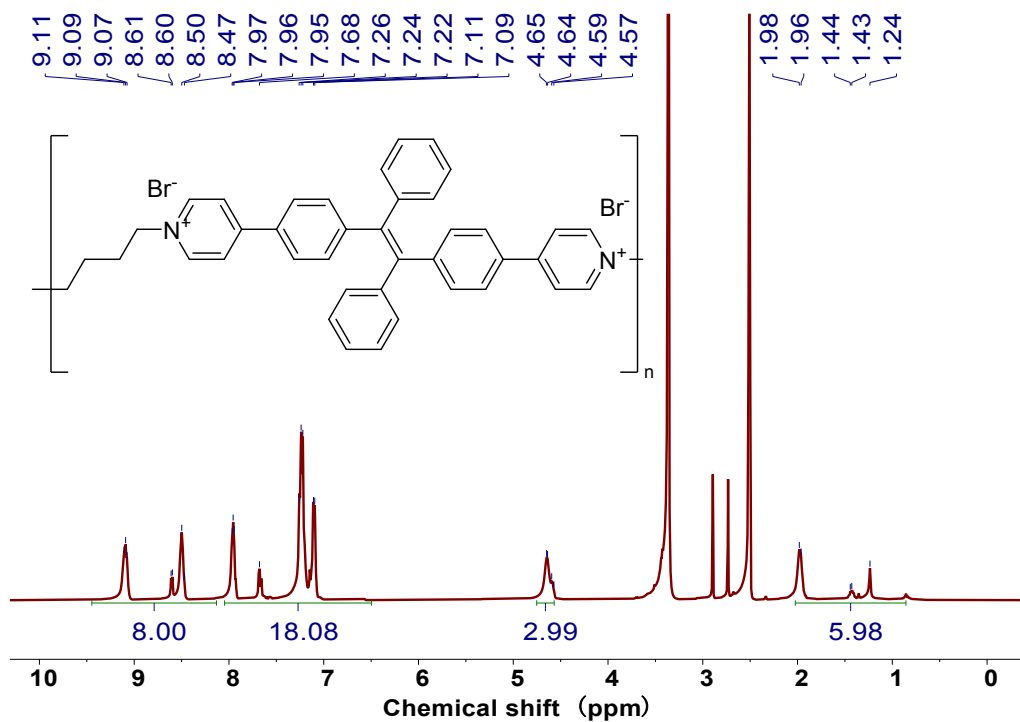


Figure S7. <sup>1</sup>H NMR spectrum of DBPE-4.

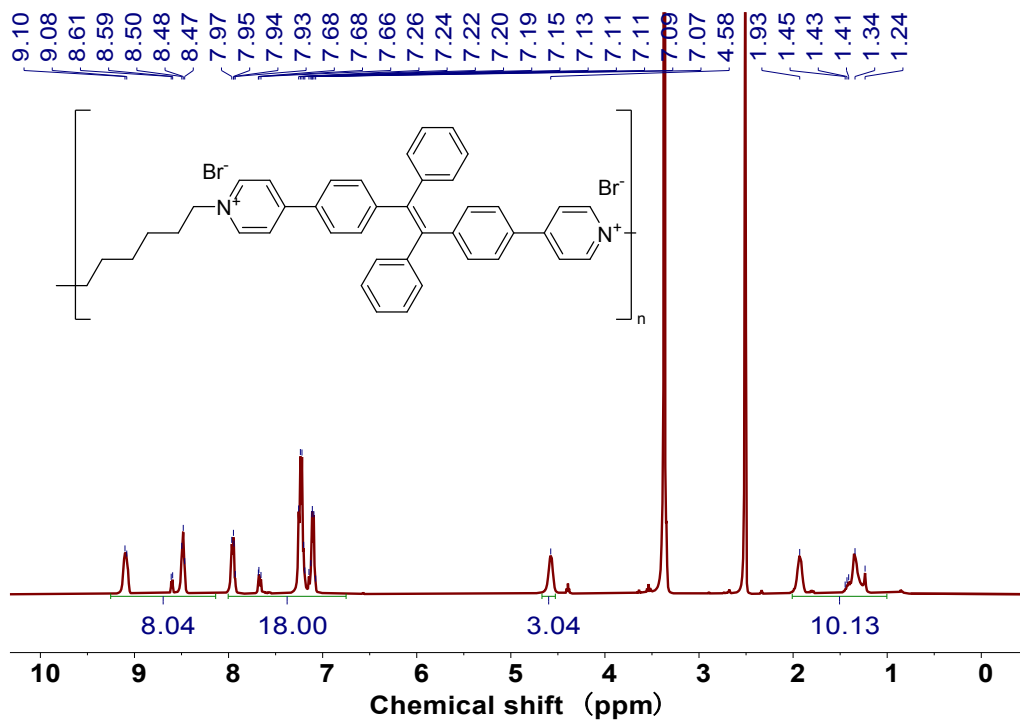


Figure S8. <sup>1</sup>H NMR spectrum of DBPE-6.

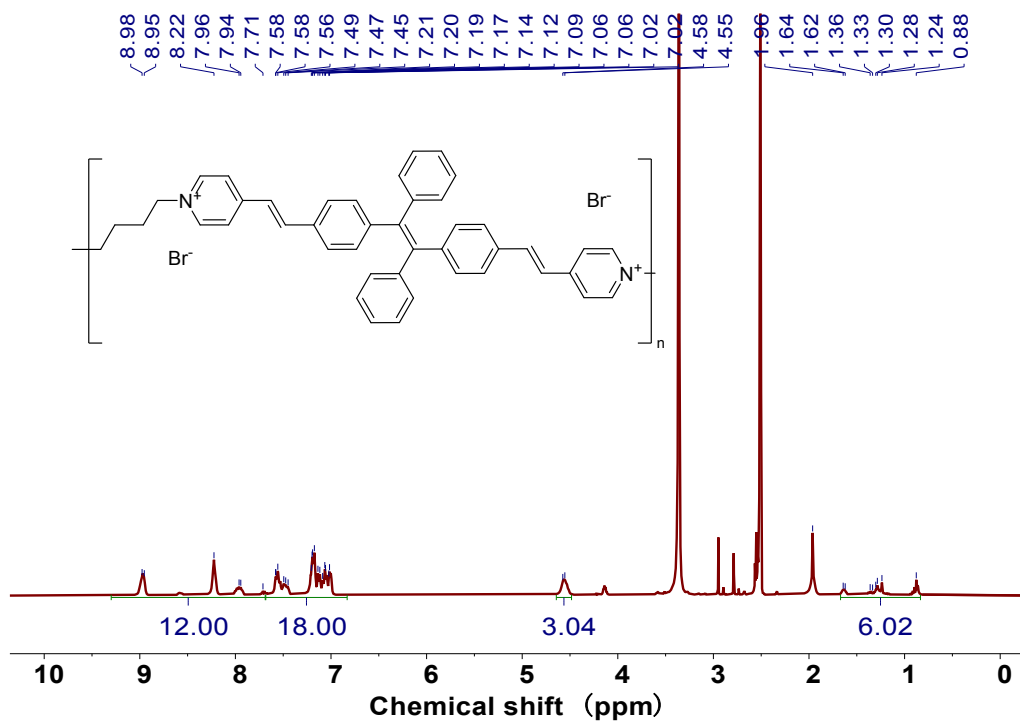


Figure S9.  $^1\text{H}$  NMR spectrum of DBPVE-4.

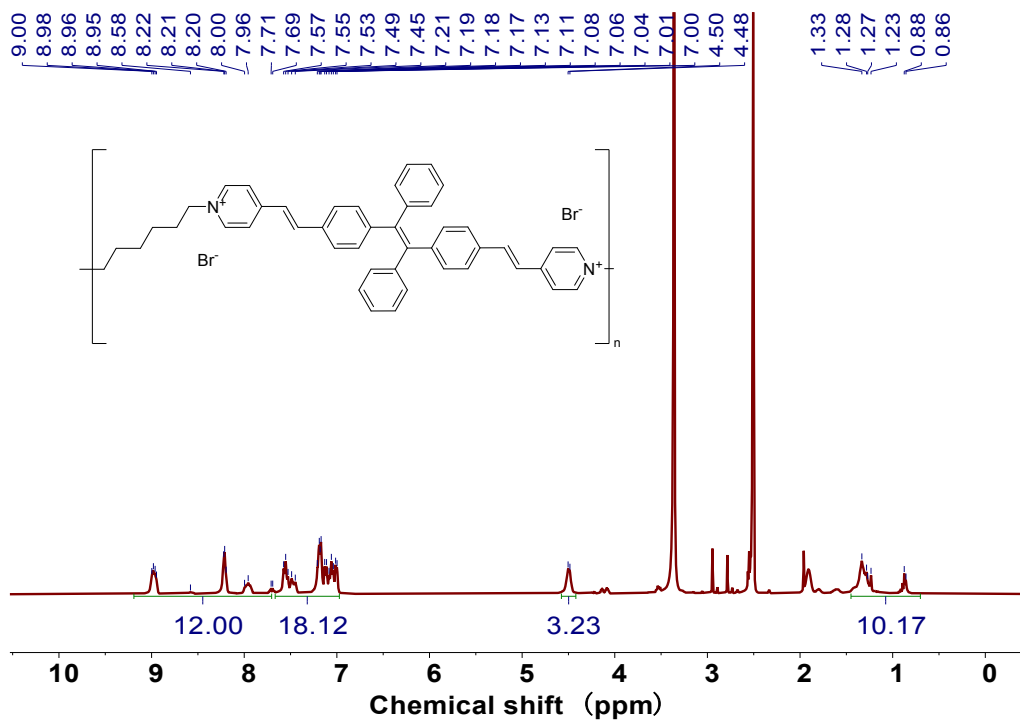


Figure S10.  $^1\text{H}$  NMR spectrum of DBPVE-6.

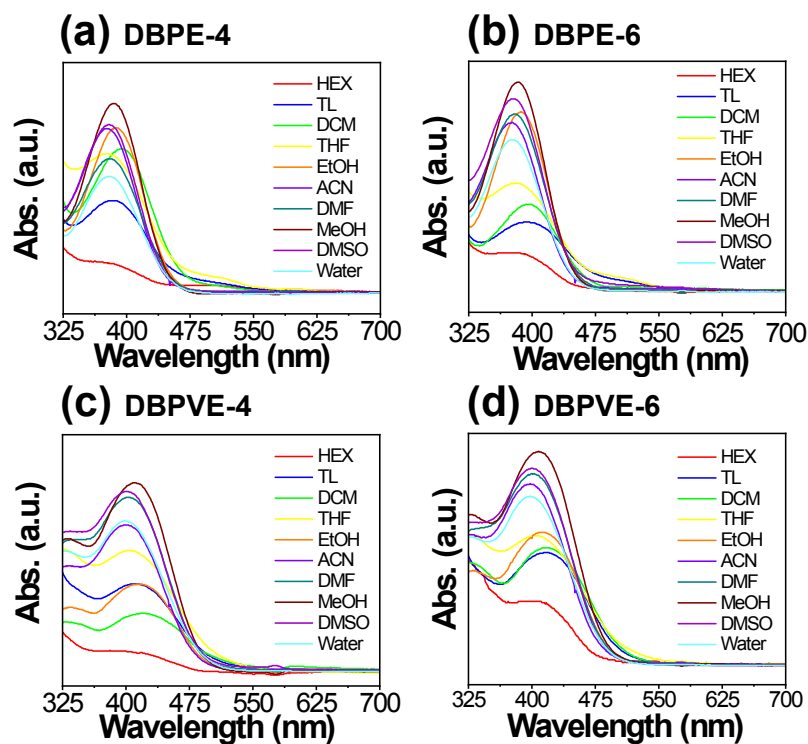


Figure S11. UV/vis spectra of DBPE-4 (a), DBPE-6 (b), DBPVE-4 (c) and DBPVE-6 (d) in different solvents. Concentration = 10  $\mu$ M.

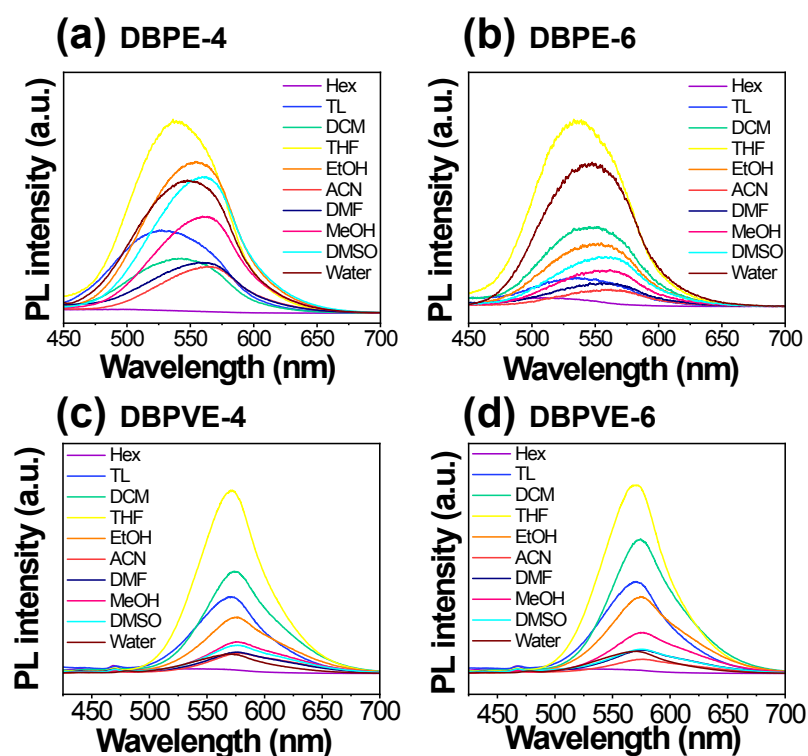
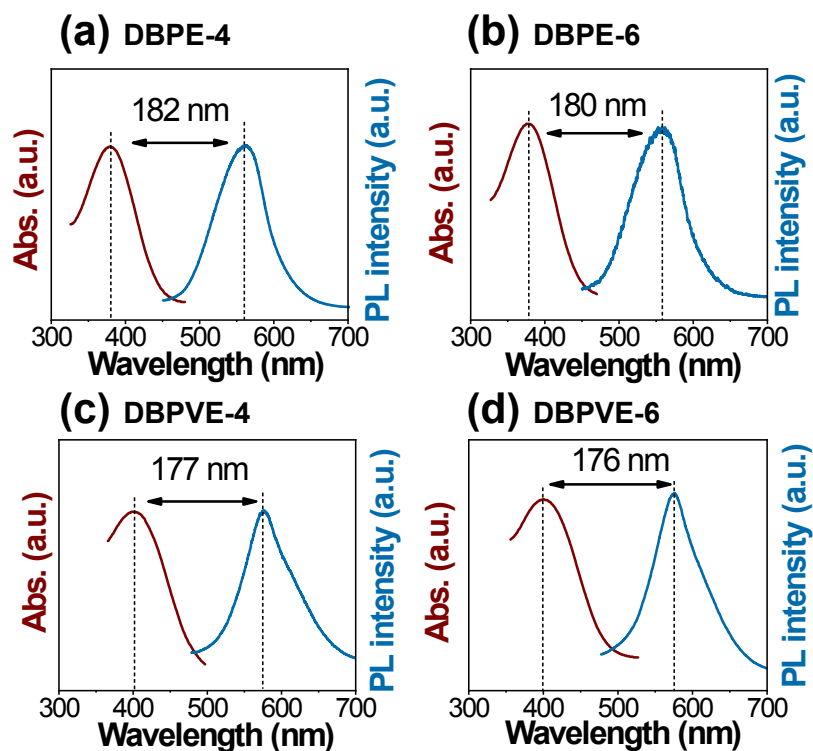
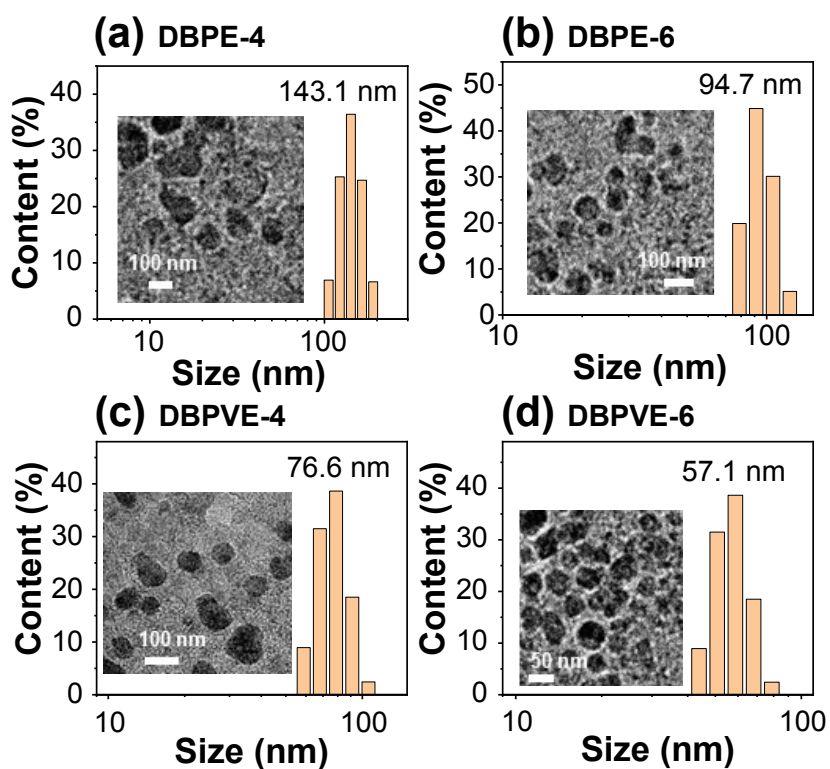


Figure S12. PL spectra of DBPE-4 (a), DBPE-6 (b), DBPVE-4 (c) and DBPVE-6 (d) in different solvents. Concentration = 10  $\mu$ M.



**Figure S13.** Stokes shift of **DBPE-4** (a), **DBPE-6** (b), **DBPVE-4** (c) and **DBPVE-6** (d) in water. Concentration = 10  $\mu\text{M}$ .



**Figure S14.** The particle size distribution and morphology of **DBPE-4** (a), **DBPE-6** (b), **DBPVE-4** (c) and **DBPVE-6** (d) by in the DMSO/water (v/v = 2/98) mixtures determined by DLS and TEM image, respectively. Concentration = 10  $\mu\text{M}$ .

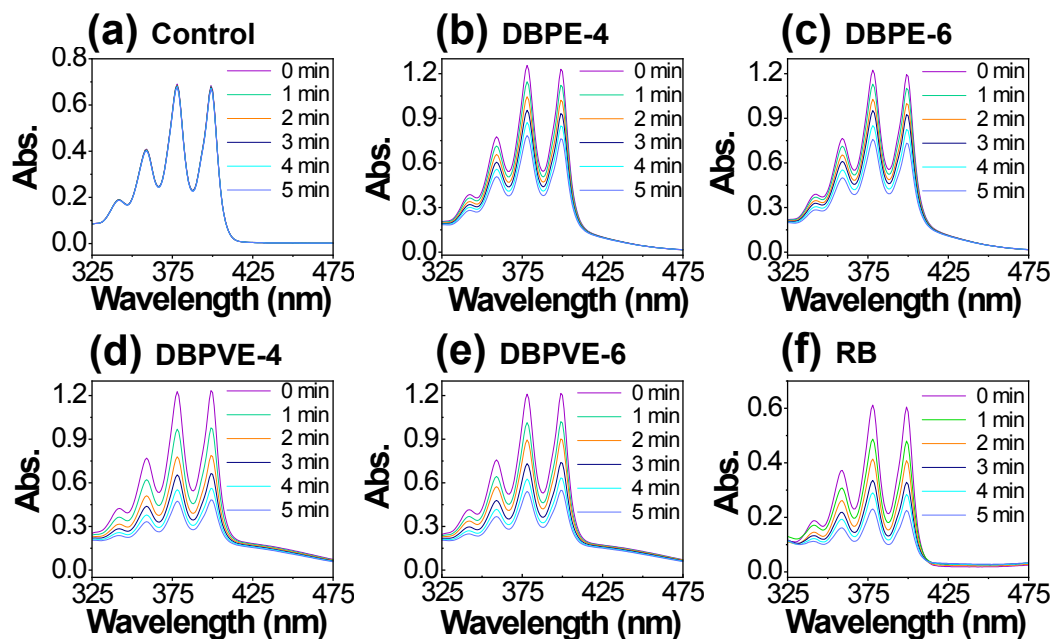


**Figure S15.** ABDA decomposition study at different time points under white light irradiation ( $60 \text{ mW cm}^{-2}$ ) for different groups, including **control group (a)**, **DBPE-4 (b)**, **DBPE-6 (c)**, **DBPVE-4 (d)**, **DBPVE-6 (e)**, and **RB (f)**. Compound concentration =  $10 \mu\text{M}$ . ABDA concentration =  $100 \mu\text{M}$ .

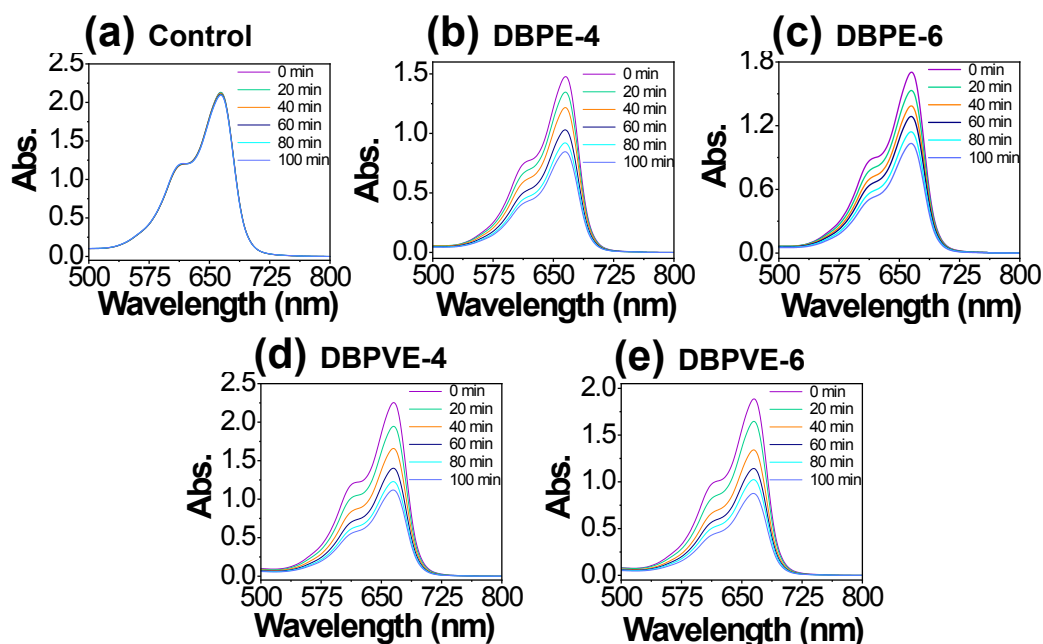


**Figure S16.** MB decomposition study at different time points under white light irradiation ( $60 \text{ mW cm}^{-2}$ ) for different groups, including **control group (a)**, **DBPE-4 (b)**, **DBPE-6 (c)**, **DBPVE-4 (d)**, and **DBPVE-6 (e)**. Compound concentration =  $10 \mu\text{M}$ . MB concentration =  $100 \mu\text{M}$ .

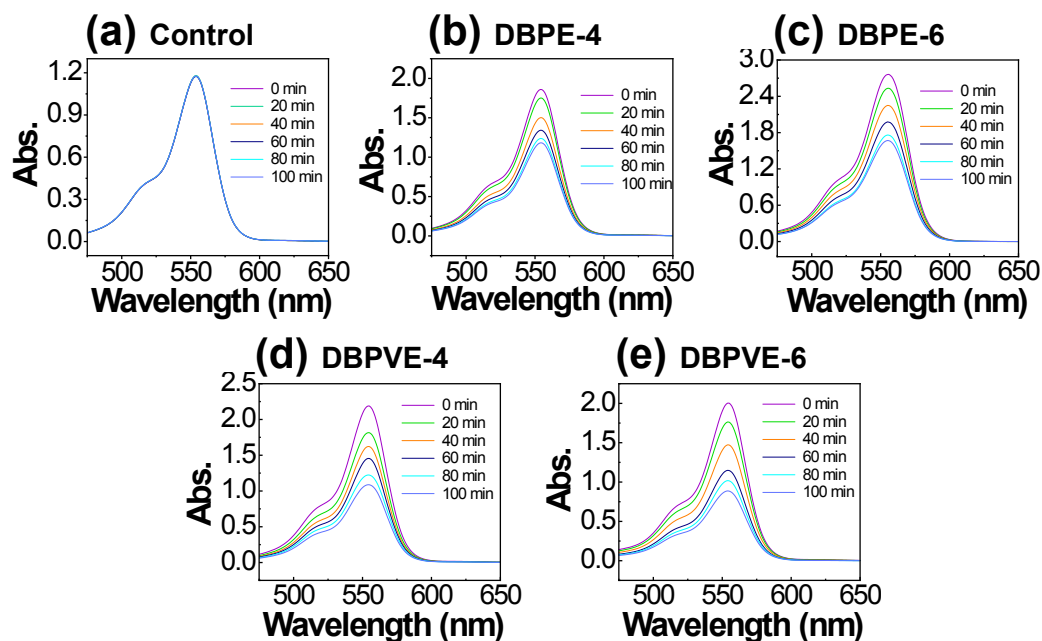


**Figure S17.** RhB decomposition study at different time points under white light irradiation (60 mW cm<sup>-2</sup>) for different groups, including **control group (a)**, **DBPE-4 (b)**, **DBPE-6 (c)**, **DBPVE-4 (d)**, and **DBPVE-6 (e)**. Compound concentration = 10 μM. RhB concentration = 100 μM.

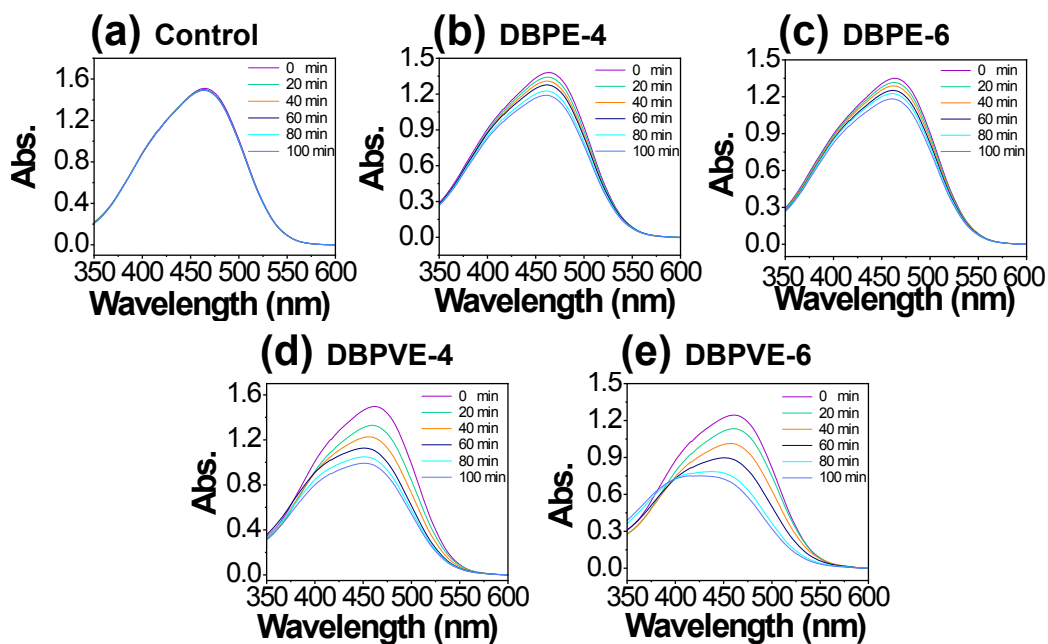


**Figure S18.** MO decomposition study at different time points under white light irradiation (60 mW cm<sup>-2</sup>) for different groups, including **control group (a)**, **DBPE-4 (b)**, **DBPE-6 (c)**, **DBPVE-4 (d)**, and **DBPVE-6 (e)**. Compound concentration = 10 μM. MO concentration = 100 μM.

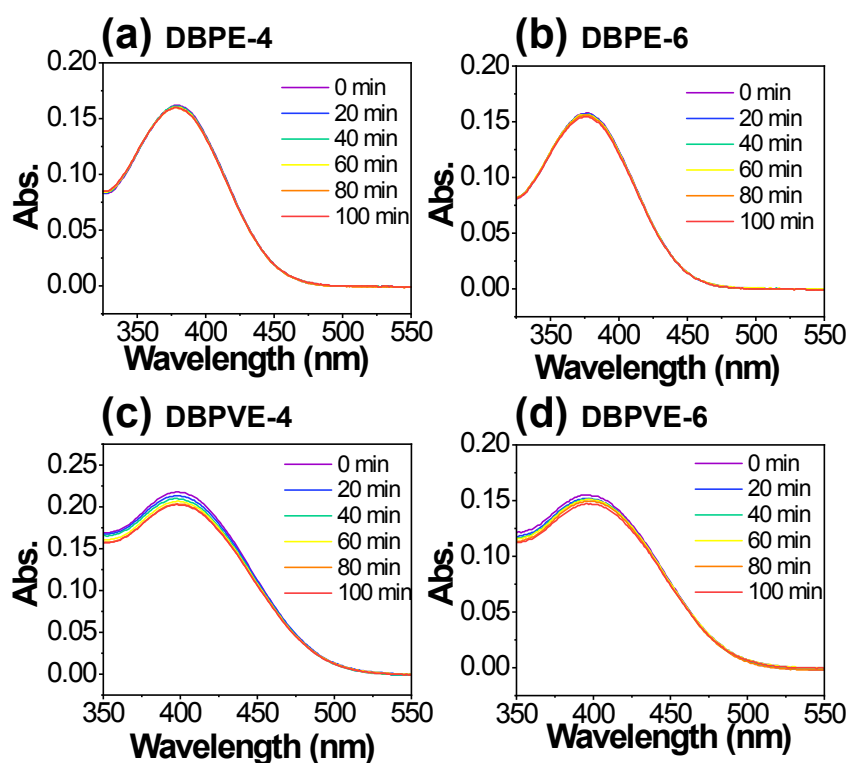


**Figure S18.** Photostability study of **DBPE-4 (a)**, **DBPE-6 (b)**, **DBPVE-4 (c)** and **DBPVE-6 (d)** by normalized UV/vis spectra in water before and after 100 min of white light irradiation ( $60 \text{ mW cm}^{-2}$ ), respectively. Concentration =  $10 \text{ }\mu\text{M}$ .

**Table S1.** Pollutant Decomposition efficiency of the Existing Photosensitizers Materials.

Photosensitizers	dye	decomposition efficiency (%)	studied conditions	ref
DBPVE-6	MB	54.1	120 min, $60 \text{ mW cm}^{-2}$	This work
	RhB	56.2		
	MO	60.4		
vis/POD/ $\text{HSO}_3^-$	MB	95	90 min, 300 W Xe	2
	RhB	95		
	MO	3		
CsPbI <sub>3</sub>	RhB	61.5	120 min, 150 W	3
	MO	50.8		

Photosensitizers	dye	decomposition efficiency (%)	studied conditions	ref
TiO <sub>2</sub> -MIL-101	MB	~33	50 min, UV-light	4
	RhB	~16		
GQDs/V-TiO <sub>2</sub>	MB	~52	32 h, 160 mW cm <sup>-2</sup>	5
MnO <sub>2</sub> /BC	MB	85	120 min, 100 mW cm <sup>-2</sup>	6
Cu <sub>2</sub> (L <sub>a</sub> )	RhB	41	45 min, UV-light	7
[ZnL <sub>c</sub> H <sub>2</sub> O] and [CdL <sub>c</sub> H <sub>2</sub> O],	RhB	51.0	6 h, 300 W Hg	8
g-C <sub>3</sub> N <sub>4</sub>	RhB	50	150 min, 100 mW cm <sup>-2</sup>	9
BW-50-AL	RhB	56	40 min, UV-light	10
PS/BODIPY 1	MO	~50	30 min, 525 mW cm <sup>-2</sup>	11
ZIF-67-600	MO	41.9	2.5 h, 300 W Xe	12
CPTF	Benzaldehyde	81.6	4 h, 100 mW cm <sup>-2</sup>	13

## Reference

1. S. S. Zhao, L. Wang, Y. Liu, L. Chen and Z. Xie, *Inorg. Chem.*, 2017, **56**, 13975-13981.
2. G. Nie and L. Xiao, *Chem. Eng.J.*, 2020, **389**, 123446.
3. M. Karami, M. Ghanbari, O. Amiri and M. Salavati-Niasari, *Sep. Purif. Technol.*, 2020, **253**, 117526.
4. N. Chang, H. Zhang, M. Shi, J. Li, C. Yin, H. Wang and L. Wang, *Microporous Mesoporous Mater.*, 2018, **266**, 47-55.
5. J. Zou, D. Wu, J. Luo, Q. Xing, X. Luo, W. Dong, S. Luo, H. Du and S. L. Suib, *ACS Catal.*, 2016, **6**, 6861-6867.
6. S. I. Siddiqui, O. Manzoor, M. Mohsin and S. A. Chaudhry, *Environ. Res.*, 2019, **171**, 328-340.
7. Y. Pan, W. Liu, D. Liu, Q. Ding, J. Liu, H. Xu, M. Trivedi and A. Kumar, *Inorg. Chem. Commun.*, 2019, **100**, 92-96.
8. F. Wang, C. Dong, C. Wang, Z. Yu, S. Guo, Z. Wang, Y. Zhao and G. Li, *New J.*

- Chem.*, 2015, **39**, 4437-4444.
9. G. Liao, S. Chen, X. Quan, H. Yu and H. Zhao, *J. Mater. Chem.*, 2012, **22**, 2721-2726.
  10. H. Ma, J. Shen, M. Shi, X. Lu, Z. Li, Y. Long, N. Li and M. Ye, *Appl. Catal. B*, 2012, **121**, 198-205.
  11. A. K. Lebechi, L. Gai, Z. Shen, T. Nyokong and J. Mack, *J. Porphyr. Phthalocyanines*, 2018, **22**, 501-508.
  12. H. Chen, K. Shen, J. Chen, X. Chen and Y. Li, *J. Mater. Chem. A*, 2017, **5**, 9937-9945.
  13. W. Wu, S. Xu, G. Qi, H. Zhu, F. Hu, Z. Liu, D. Zhang and B. Liu, *Angew. Chem. Int. Ed.*, 2019, **58**, 3062-3066.